

# Prototype Refinement Network for Few-Shot Segmentation

Jinlu Liu , Yongqiang Qin

AInnovation Technology Co., Ltd.

{liujinlu, qinyongqiang}@ainnovation.com

## Abstract

Few-shot segmentation targets to segment new classes with few annotated images provided. It is more challenging than traditional semantic segmentation tasks that segment pre-defined classes with abundant annotated data. In this paper, we propose Prototype Refinement Network (PRNet) to attack the challenge of few-shot segmentation. PRNet learns to bidirectionally extract prototypes from both support and query images, which is different from existing methods. To extract representative prototypes of the new classes, we use *adaptation* and *fusion* for prototype refinement. The adaptation of PRNet is implemented by fine-tuning on the support set. Furthermore, prototype fusion is adopted to fuse support prototypes with query prototypes, incorporating the knowledge from both sides. Refined in this way, the prototypes become more discriminative in low-data regimes. Experiments on PASAL-5<sup>i</sup> and COCO-20<sup>i</sup> demonstrate the superiority of our method. Especially on COCO-20<sup>i</sup>, PRNet significantly outperforms previous methods by a large margin of 13.1% in 1-shot setting and 17.4% in 5-shot setting respectively.

## 1 Introduction

Significant breakthroughs have been made in semantic segmentation tasks by taking the benefits of strong feature learning ability of deep neural networks [Simonyan and Zisserman, 2015; He *et al.*, 2016]. Various networks were proposed for semantic segmentation problems, such as FCN [Long *et al.*, 2015], RefineNet [Lin *et al.*, 2017] and DeepLab series [Chen *et al.*, 2018a; Chen *et al.*, 2017; Chen *et al.*, 2018b]. And besides, the availability of large-scale dataset is another key issue of the breakthroughs. The performance is severely dependent on the training data which requires a large number of pixel-level annotations. However, pixel-level annotations are difficult and expensive to obtain and furthermore, training with abundant data makes the model hard to generalize to new categories with only few labeled data. It arouses the interest of learning a model that can segment a new concept from few samples, which is so-called few-shot segmentation.

In a  $N$ -way  $K$ -shot segmentation task, we target to segment the query images given  $K$  annotated support images from each of the  $N$  classes. Prototype based methods are widely used in handling few-shot tasks like classification [Snell *et al.*, 2017] and segmentation [Dong and Xing, 2018; Wang *et al.*, 2019]. For few-shot segmentation, prototype based methods treat it as a classification problem that classifies each pixel to the class of the nearest prototype. Existing methods [Dong and Xing, 2018; Wang *et al.*, 2019] put emphasis on learning representative prototypes which are closer to the pixels belonging to the same semantic class in the feature space. However, in few-shot segmentation, prototypes directly extracted from the support images are usually biased to represent the semantic classes in the query images, due to the data scarcity and large intra-class variance. Therefore, we are encouraged to refine the prototypes to be more representative for segmentation.

In this paper, we propose Prototype Refinement Network (PRNet) for few-shot segmentation. The proposed method mainly consists of two parts: prototype learning and prototype refinement. At the training stage, PRNet learns to extract prototypes from both support images and query images, which is different from most methods that merely extract prototypes from the support set. Images are input to the network embedded as the deep features and we obtain the support prototypes by masked average pooling on the support features. Then, the segmentation mask of the query image is predicted by nearest prototype matching of the query feature at each spatial location. Given the predicted mask, we also compute query prototypes to segment the support images in the same way. The bidirectional constraints drive the network to extract representative support prototypes that can precisely segment the query images and vice versa.

At the test stage, it requires the network to perform segmentation on the classes that are unseen during training. To extract more representative prototypes, we implement *adaptation* and *fusion* for prototype refinement as shown in Figure 1. The feature extractor is tuned on the few support images to adapt to the unseen classes. For adaptation, the support prototypes are extracted to segment the support images which is different from the practice in training. Furthermore, we propose a two-stage fusion method that fuses the support prototypes with the query prototypes for refinement. We compute similarity maps where the confidently segmented regions are

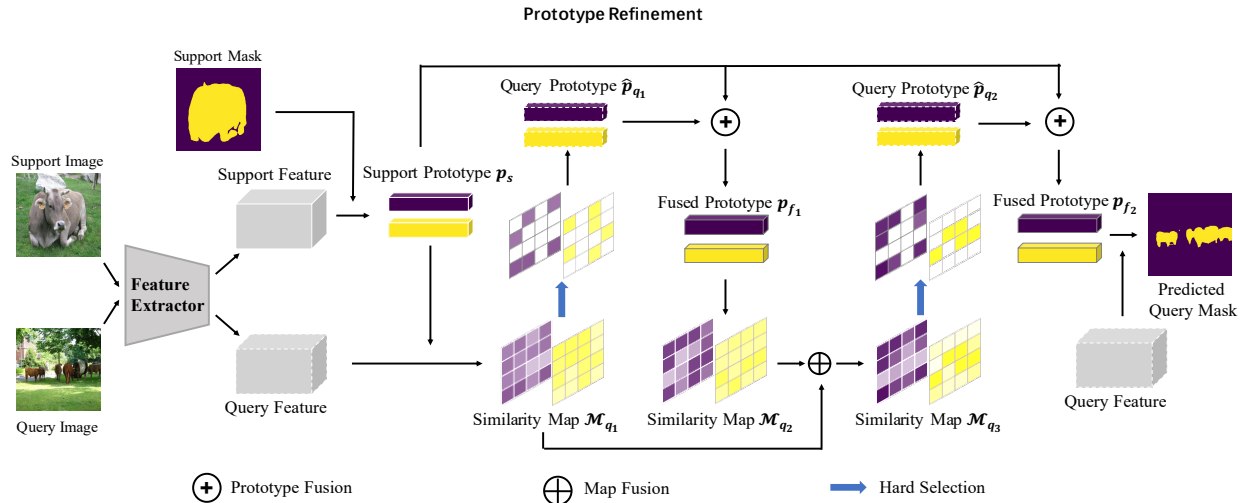


Figure 1: We take a 1-way 1-shot segmentation task for example to illustrate our prototype refinement network. *Adaptation* and *fusion* are used for prototype refinement. The feature extractor is adapted to the support set for prototype extraction. And we fuse support prototypes with predicted query prototypes as the final prototypes for segmentation. Color shades in the map indicate the similarity degree. Best viewed in color.

identified by a self-adaptive threshold  $\alpha$ . The query prototypes  $\hat{p}_{q_1}$  are accordingly extracted from the spatial locations that are included in the selected regions. As displayed in Figure 1, the fused prototype  $p_{f_1}$  is firstly formed by support prototypes  $p_s$  and query prototypes  $\hat{p}_{q_1}$ . Given  $p_{f_1}$ , we compute new similarity maps, obtaining new prototypes  $\hat{p}_{q_2}$  after map fusion and hard selection. Then we implement fusion the second time by fusing  $p_{f_1}$  with  $\hat{p}_{q_2}$ . In this way, the discriminative knowledge of the query images is introduced for prototype extraction. Prototype fusion is an efficient method for refinement without introducing extra learnable parameters at testing. We conduct experiments on PASCAL-5<sup>i</sup> and COCO-20<sup>i</sup>, finding that our proposed PRNet brings in obvious improvement by a large margin.

Our contributions are summarized as:

- 1) We propose prototype refinement network for few-shot segmentation, which effectively explores the representative prototypes and performs segmentation by nearest prototype matching.
- 2) We demonstrate the effectiveness and simplicity of the proposed fusion method that can significantly improve the performance without importing extra learnable parameters. The fused prototypes are more representative in few-shot scenarios.
- 3) We achieve the state-of-the-art results on both PASCAL-5<sup>i</sup> and COCO-20<sup>i</sup>. Especially on COCO-20<sup>i</sup>, we consistently outperform existing methods in all cases with the increase of mean-IoU score up to 17.4%.

## 2 Related Works

**Semantic Segmentation** classifies each pixel in an image into several pre-defined classes. Abundant approaches are exploited for pixel-wise segmentation tasks such as FCN [Long *et al.*, 2015], UNet [Ronneberger *et al.*, 2015] and

DeepLab series [Chen *et al.*, 2018a; Chen *et al.*, 2017; Chen *et al.*, 2018b]. Dilated convolution [Yu and Koltun, 2016] is widely adopted in segmentation tasks to increase receptive fields which is also used in our methods.

**Few-Shot Learning** aims to predict image labels with few support samples provided. Existing methods are commonly divided into two branches: meta-learning based methods [Finn *et al.*, 2017; Nichol and Schulman, 2018] and metric learning based methods [Snell *et al.*, 2017; Allen *et al.*, 2019]. MAML [Finn *et al.*, 2017] is a typical meta-learning method which targets to learn a good weight initialization from small support samples, enabling fast adaptation to new tasks by a few gradient steps. PN [Snell *et al.*, 2017] is a typical metric learning method which achieves classification by finding the nearest class prototype in the embedding space.

**Few-Shot Segmentation** is a new task that attacks the semantic segmentation problem in few-shot scenarios. It requires to perform pixel-wise segmentation from few annotated images available. Previous approaches adopt two-branch architectures to align support images with query images [Shaban *et al.*, 2017; Zhang *et al.*, 2018; Wang *et al.*, 2019; Hu *et al.*, 2019]. OLSM [Shaban *et al.*, 2017] was proposed for one-shot semantic segmentation which uses support branch to learn parameters for the logistic regression layer of the query branch. Similar idea of weight learning was adopted in AMP [Siam *et al.*, 2019] which uses the support feature after masked average pooling to imprint the 1x1 convolutional filters of the final segmentation layer of the query image. Prototype learning based methods [Dong and Xing, 2018; Wang *et al.*, 2019] were recently proposed for few-shot segmentation. PANet [Wang *et al.*, 2019] viewed the averaged features as prototypes and trained the feature extractor by adding alignment constraints between support prototypes and query prototypes. Our method is similar to PANet but we fur-

ther propose the prototype refinement approach to make prototypes more suitable to represent the target classes in low-data regimes.

### 3 Methods

Our proposed method mainly consists of two stages: prototype learning and prototype refinement, which correspond to the training and test stages accordingly. The network firstly learns from the training classes to extract class prototypes from both support set and query set, which is different from most previous methods. When testing on the test classes, we tune the feature extractor to adapt to the support set and then, we use prototype fusion for further refinement. The prototypes refined in this way are more representative in few-shot scenarios.

#### 3.1 Problem Definition

In few-shot segmentation, a dataset  $\mathcal{D}_{train}$  of classes  $\mathcal{C}_{train}$  is given for training the segmentation network. Then the network is required to perform segmentation on the set  $\mathcal{D}_{test}$  of classes  $\mathcal{C}_{test}$  which have no overlap with  $\mathcal{C}_{train}$ . Both datasets are composed of  $N$ -way  $K$ -shot segmentation tasks, denoted as  $\mathcal{D}_{train} = \{\mathcal{T}_i = (\mathcal{S}_i, \mathcal{Q}_i)\}_{i=1}^{I_{train}}$  and  $\mathcal{D}_{test} = \{\mathcal{T}_i = (\mathcal{S}_i, \mathcal{Q}_i)\}_{i=1}^{I_{test}}$ . In each task, the model learns from the support set  $\mathcal{S}_i = \bigcup_{n=1}^N \{(I_s^{n,k}, M_s^{n,k})\}_{k=1}^K$  where each of  $N$  classes has  $K$  support images  $I_s$  paired with ground-truth segmentation masks  $M_s$ . And the model need to segment the images in the query set  $\mathcal{Q}_i = \{(I_q^t, M_q^t)\}_{t=1}^T$  where  $T$  is the total number of the query images in a task. At the training stage, we train our network on the tasks sampled from  $\mathcal{D}_{train}$  while at the test stage, we evaluate it on the tasks from  $\mathcal{D}_{test}$ .

#### 3.2 Prototype Learning

The general idea of existing prototypical networks [Snell *et al.*, 2017; Dong and Xing, 2018; Wang *et al.*, 2019] is representing categories by the learnt feature vectors which are viewed as prototypes in the feature space. According to it, pixel-wise segmentation can be performed by labeling every pixel with the semantic class of the nearest prototype. Inspired by [Wang *et al.*, 2019], we train the model by bidirectionally learning prototypes from both support images and query images. Support and query images are first input to the network  $f_\theta$  embedded as the deep features. Based on the features, support prototypes of foreground classes are computed by masked average pooling  $MAP(\cdot)$  which are denoted as:

$$\begin{aligned} p_s^n &= \frac{1}{K} \sum_{k=1}^K MAP(f_\theta(I_s^{n,k}), M_s^{n,k}) \\ &= \frac{1}{K} \sum_{k=1}^K \frac{\sum_{x,y} F_{s;x,y}^{n,k} [\mathbb{1}(M_{s;x,y}^{n,k} = n)]}{\sum_{x,y} \mathbb{1}(M_{s;x,y}^{n,k} = n)} \end{aligned} \quad (1)$$

where  $F_s^{n,k}$  is the extracted support feature and  $(x, y)$  is the spatial location in the feature. Background is also treated as a semantic class whose prototype  $p_s^0$  is computed by feature averaging of all spatial locations excluded in any foreground

classes. Given the support prototypes  $\{p_s^n\}_{n=0}^N$  of  $N$  foreground classes and the background, we perform segmentation by distance computation between the query features at each spatial location and the support prototypes. The segmentation mask  $\hat{M}_q$  of the query image is predicted pixel by pixel as follows:

$$\begin{aligned} \hat{M}_{q;x,y}^t &= \arg \max_n \mathcal{M}_q^{t,n} \\ &= \arg \max_n \sigma(d(F_{q;x,y}^t, p_s^n)) \end{aligned} \quad (2)$$

where  $F_{q;x,y}^t$  is the feature vector of query image  $I_q^t$  at the location  $(x, y)$  and  $d(\cdot)$  is the distance function which is the cosine distance adopted in this paper. If the query image is correctly segmented, there should be query prototypes extracted accordingly that can segment the support images as described above. Therefore, we extract query prototypes  $\hat{p}_q$  based on the predicted mask  $\hat{M}_q$  and perform segmentation on the support images as follows:

$$\hat{p}_q = \frac{1}{T} \sum_{t=1}^T MAP(f_\theta(I_q^t), \hat{M}_q^t) \quad (3)$$

$$\hat{M}_s = \arg \max_n \sigma(d(F_s^k, \hat{p}_q^n)) \quad (4)$$

The network is trained end-to-end by the objective:

$$\mathcal{L}_{train} = \mathcal{L}_{CE}(M_s, \mathcal{M}_s) + \mathcal{L}_{CE}(M_q, \mathcal{M}_q) \quad (5)$$

where  $\mathcal{L}_{CE}(\cdot)$  is the standard cross-entropy loss. Most methods [Dong and Xing, 2018; Zhang *et al.*, 2019] only regulate the network to perform segmentation on the query set which corresponds to the second term in Eq. 5. Different with them, we regulate the network from both sides as indicated in Eq. 5. In this way, the network is driven to learn an efficient feature space where the prototypes are more representative to the semantic classes.

#### 3.3 Prototype Refinement

Since the test classes  $\mathcal{C}_{test}$  are unseen at the training stage, the prototypes directly extracted from few support images are inevitably to be biased. It is to say that the support prototypes are less capable of representing the semantic class due to the data scarcity and class variance. Therefore, we propose to refine class prototypes at the test stage by two ways: adaptation and fusion.

**Adaptation** Since  $\mathcal{C}_{test}$  remains unseen to the feature extractor  $f_\theta$  before testing, it is necessary to adapt  $f_\theta$  to  $\mathcal{D}_{test}$  for discriminative feature extraction. Fine-tuning a meta-trained model on a few-shot set is verified to achieve strongly competitive performance in few-shot scenarios [Dhillon *et al.*, 2020]. Referring to it, we fine-tune the feature extractor on the support set by the following objective:

$$\mathcal{L}_{adapt} = \mathcal{L}_{CE}(M_s, \mathcal{M}_s) \quad (6)$$

where  $\mathcal{M}_s = \sigma(d(F_s, p_s))$ . Notably, different from the practice at the prototype learning stage, we use support prototypes to segment support images as indicated in Eq. 6. By fine-tuning on the support set, the feature extractor can learn

more discriminative features which the prototypes are extracted from.

**Fusion** Due to the data scarcity and large intra-class variance in few-shot scenarios, the support prototypes are not representative enough in the embedding space. Thus, the pixels in query images are easily to be misclassified by non-parametric distance computation with support prototypes. To make the prototypes be more representative, we propose a two-step fusion method for further prototype refinement. The framework of prototype fusion is shown in the right part of Figure 1. Given the support prototypes  $p_s$ , we compute cosine similarity map  $\mathcal{M}_{q_1}$  of each query image by dense comparison with  $p_s$  at each spatial location and predict the query mask  $\hat{M}_{q_1}$ . Similar to the practice at the prototype learning stage, query prototypes can be extracted accordingly. However, the rough segmentation of query image will result in the inefficiency of the extracted query prototypes. Thus we apply hard selection  $\mathcal{H}(\cdot)$  with a self-adaptive threshold  $\alpha$  to segment high-confident regions, which is to say that, locations with cosine similarity larger than  $\alpha$  are considered to be correctly segmented. The selected locations form the sparse query mask  $\mathcal{H}(\mathcal{M}_{q_1})$  that is used for masked average pooling to extract query prototype  $p_{q_1}$  as follows:

$$\hat{p}_{q_1} = \frac{1}{T} \sum_{t=1}^T MAP(f'_\theta(I_q^t), \mathcal{H}(\hat{M}_{q_1}^t, \mathcal{M}_{q_1}^t)) \quad (7)$$

where  $f'_\theta$  is the adapted feature extractor. The hard selected is implemented by:

$$\mathcal{H}(\hat{M}_{q_1}^t, \mathcal{M}_{q_1}^t)_{x,y} = \begin{cases} \hat{M}_{q_1}^t_{x,y} & \text{if } \mathcal{M}_{q_1}^t_{x,y} > \alpha^n \\ -1 & \text{otherwise} \end{cases} \quad (8)$$

where the value  $-1$  indicates the location not belonging to any foreground classes and background and  $n = \arg \max_j \mathcal{M}_{q_1}^t_{x,y}^j$  where  $j = 0, \dots, N$ . The value of threshold  $\alpha^n$  of each class is given in Section 4. Then we fuse support prototype  $p_s$  with query prototype  $\hat{p}_{q_1}$  by Eq. 9:

$$p_{f_1} = \omega_s p_s + \omega_q \hat{p}_{q_1} \quad (9)$$

where  $\omega_s$  and  $\omega_q$  are hyper-parameters that control the fusion weights. After obtaining the fused prototypes  $p_{f_1}$ , we compute the similarity map  $\mathcal{M}_{q_2}$  and apply map fusion on  $\mathcal{M}_{q_1}$  and  $\mathcal{M}_{q_2}$  to get the final map:

$$\mathcal{M}_{q_3} = (\mathcal{M}_{q_1} + \mathcal{M}_{q_2})/2 \quad (10)$$

The predicted mask  $\hat{M}_{q_2}$  is obtained as aforementioned. We query prototypes  $\hat{p}_{q_2}$  are computed by:

$$\hat{p}_{q_2} = \frac{1}{T} \sum_{t=1}^T MAP(f'_\theta(I_q^t), \mathcal{H}(\hat{M}_{q_2}^t, \mathcal{M}_{q_3}^t)) \quad (11)$$

We again implement prototype fusion on  $p_{f_1}$  and  $\hat{p}_{q_2}$  as:

$$p_{f_2} = \omega_f p_{f_1} + \omega_q \hat{p}_{q_2} \quad (12)$$

Based on the refinement implemented so far, we utilize the fused prototype  $p_{f_2}$  as the final prototype to segment the query image.

It can be seen that the prototypes  $p_{f_2}$  fuse the knowledge from both support prototypes and query prototypes, which enjoy the advantage of both sides. On the one hand, retaining the knowledge of support images avoids overfitting when segmenting the query images. On the other hand, importing the knowledge from query images makes the prototype be more discriminative. Our refinement strategy is easy to implement, refrained from tuning many hyper-parameters. The fusion weights are all set to 0.5 in this paper. Different weights do not make a substantial difference therefore, we do not fine tune the weights in our experiments. Our method has a stable performance which is free from carefully tuning the hyper-parameters. Subsequent experiments in Section 4 verify the effectiveness of the proposed adaptation and prototype fusion.

## 4 Experiments

### 4.1 Setup

**Datasets** We evaluate our method on two few-shot segmentation benchmarks: PASCAL-5<sup>i</sup> [Shaban *et al.*, 2017] and COCO-20<sup>i</sup> [Nguyen and Todorovic, 2019]. PASCAL-5<sup>i</sup> is a derivation of PASCAL VOC 2012 [Everingham *et al.*, 2010] which is split into 4 folds. Each fold contains 5 categories. COCO-20<sup>i</sup> is a larger dataset which is derived from MS COCO [Lin *et al.*, 2014]. 80 categories are divided into 4 folds with each fold containing 20 categories. Two splits are adopted in our experiments which are split-A proposed in [Nguyen and Todorovic, 2019] and split-B [Hu *et al.*, 2019] respectively. In few-shot segmentation, models are trained on three folds and evaluated on the rest fold.

**Evaluation Protocols** We use mean-IoU and binary-IoU for evaluation which are commonly adopted in few-shot segmentation settings. Mean-IoU measures the average IoU score of all foreground classes. Binary-IoU treats all foreground objects as one class and the background is viewed as one class.

**Implementation Details** We modify ResNet 101 [He *et al.*, 2016] as feature extractor in our experiments. Following the previous works [Shaban *et al.*, 2017; Wang *et al.*, 2019], the base network is initialized by the pretrained weights on ILSVRC [Russakovsky *et al.*, 2015]. The network is trained end-to-end by SGD with learning rate of  $7e-3$ , momentum of 0.9 and weight decay of  $5e-4$ . We train 30,000 iterations for each model and the learning rate is reduced by 0.1 every 10,000 iterations. Horizontal flipping is used for data augmentation. The number of query images in each episode is set to 1 in all experiments. At the test stage, most previous methods randomly sample 1,000 episodes for evaluation but the results vary greatly with different random seeds. To give a reliable and stable result, we follow [Wang *et al.*, 2019] to report the average result of 5 runs.

**Threshold** The threshold  $\alpha$  of each class is self-adaptively computed by:

$$\alpha^n = (V_{max}^n + V_{mean}^n)/2 \quad (13)$$

$$V_{max}^n = \max\{V_{x,y}^n\}; V_{mean}^n = \text{mean}\{V_{x,y}^n\} \quad (14)$$

Methods	1-shot					5-shot				
	fold-1	fold-2	fold-3	fold-4	Mean	fold-1	fold-2	fold-3	fold-4	Mean
OSLSM [Shaban <i>et al.</i> , 2017]	33.60	55.30	44.90	33.50	40.80	35.90	58.10	42.70	39.10	43.90
co-FCN [Rakelly <i>et al.</i> , 2018]	36.70	50.60	44.90	32.40	41.10	37.50	50.00	44.10	33.90	41.40
SG-One [Zhang <i>et al.</i> , 2018]	40.20	58.40	48.40	38.40	46.30	41.90	58.60	48.60	39.40	47.10
PANet [Wang <i>et al.</i> , 2019]	42.30	58.00	51.10	41.20	48.10	51.80	64.60	59.80	46.50	55.70
AMP [Siam <i>et al.</i> , 2019]	41.90	50.20	46.7	34.7	43.40	41.80	55.50	50.30	39.90	46.90
CANet [Zhang <i>et al.</i> , 2019]	52.50	65.90	51.30	51.90	55.40	55.50	67.80	51.90	53.20	57.10
FWB [Nguyen and Todorovic, 2019]	51.30	64.69	56.71	52.24	<b>56.19</b>	54.84	67.38	62.16	55.30	59.92
PRNet (ours)	51.60	61.32	53.10	47.59	53.40	57.84	67.31	64.08	53.36	<b>60.56</b>

Table 1: Mean-IoU results on PASCAL-5<sup>i</sup>.

Methods	Split	1-shot					5-shot				
		fold-1	fold-2	fold-3	fold-4	Mean	fold-1	fold-2	fold-3	fold-4	Mean
PANet [Wang <i>et al.</i> , 2019]	A	-	-	-	-	20.90	-	-	-	-	29.70
PRNet (ours)		41.16	26.28	24.74	21.92	<b>28.53</b>	50.37	32.85	31.77	29.14	<b>36.03</b>
FWB [Nguyen and Todorovic, 2019]	B	16.98	17.98	20.96	28.85	21.19	19.13	21.46	23.93	30.08	23.65
PRNet (ours)		33.59	37.39	33.64	32.53	<b>34.29</b>	40.44	44.43	39.41	39.91	<b>41.05</b>

Table 2: Mean-IoU results on COCO-20<sup>i</sup>. Split-A and split-B are two different setups for 4-fold cross-validation on COCO-20<sup>i</sup>.

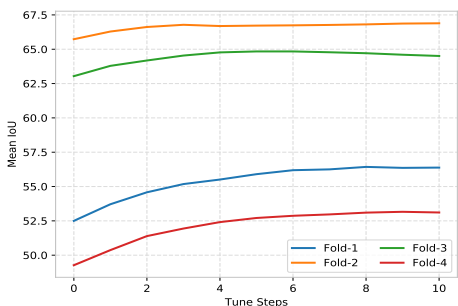


Figure 2: The mean-IoU results of different tune steps on 5-shot PASCAL-5<sup>i</sup>.

where  $\{V_{x,y}^n\}$  are cosine similarity values of the locations  $(x, y)$  that are segmented as class  $n$ .

**Network** We modify the ResNet 101 [He *et al.*, 2016] network as our feature extractor. The first two blocks remain unchanged. The strides of last two blocks are set to 1. To enlarge the reception field, we use dilated convolutions with rates of 2 and 4 in the last two blocks. Layers after the 4-th block are removed and, the last ReLU layer in the last block is removed.

## 4.2 1-way Segmentation

**PASCAL-5<sup>i</sup>** Table 1 shows the mean-IoU results on PASCAL-5<sup>i</sup>. Compared with the prototype learning method PANet, we generally outperform it by a margin of 5%. Our PRNet achieves the best performance in the 5-shot setting. However, in the 1-shot setting, our result is relatively lower than CANet and FWB. One possible reason is that the adaptation step plays a limited role in the 1-shot tasks, resulting in small improvements. The binary-IoU scores on PASCAL-5<sup>i</sup> are displayed in Table 4. We can see that our method shows the best performance evaluated by binary-IoU.

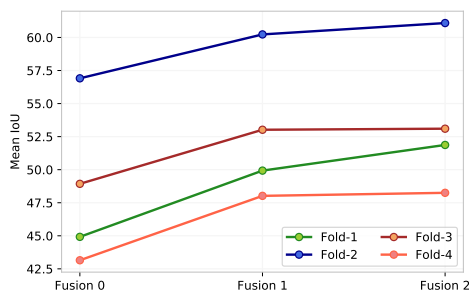


Figure 3: Prototype Fusion: mean-IoU in 1-shot setting on PASCAL-5<sup>i</sup>. Fusion 0: without prototype fusion. Fusion 1: with one-stage prototype fusion. Fusion 2: with two-stage prototype fusion.

**COCO-20<sup>i</sup>** Table 2 compares our method with PANet and FWB on COCO-20<sup>i</sup> in different splits. It is obvious to see that our PRNet consistently outperforms the state-of-the-art methods on all folds. COCO-20<sup>i</sup> is a more challenging dataset that contains more categories and the quality of segmentation mask is relatively lower. However, our PRNet achieves significant improvements by a large margin especially in split-B. We outperform FWB by a margin of 13% in 1-shot task and 18% in 5-shot task. To give a comprehensive evaluation of our method, we give the binary-IoU results of two splits in Table 5. It further demonstrate the effectiveness of our method that performs best in all cases.

## 4.3 Analysis

**Adaptation** The results of adaptation are shown in Figure 2 which are computed from 1 run of 1,000 randomly sampled episodes in each fold. The adaptation yields consistent improvement with increasing steps and the overall performance reaches the summit after 5 steps. We find that mean-IoU score in fold 3 drops slightly after 5 steps which reveals the risk of

Methods	1-shot					5-shot				
	fold-1	fold-2	fold-3	fold-4	Mean	fold-1	fold-2	fold-3	fold-4	Mean
SG-One [Zhang <i>et al.</i> , 2018]	-	-	-	-	-	-	-	-	-	29.4
PANet [Wang <i>et al.</i> , 2019]	-	-	-	-	45.1	-	-	-	-	53.1
PRNet <sub>fusion</sub>	43.49	55.24	48.32	39.92	<b>46.74</b>	52.64	60.67	56.9	48.16	<b>54.59</b>

Table 3: 2-way Segmentation: mean-IoU score on PASCAL-5<sup>i</sup>. In this experiment, we only use fusion for refinement without adaptation.

Methods	1-shot	5-shot
OSLSM [Shaban <i>et al.</i> , 2017]	61.3	61.5
co-FCN [Rakelly <i>et al.</i> , 2018]	60.1	60.2
PL [Dong and Xing, 2018]	61.2	62.3
A-MCG [Hu <i>et al.</i> , 2019]	61.2	62.2
SG-One [Zhang <i>et al.</i> , 2018]	63.9	65.9
AMP [Siam <i>et al.</i> , 2019]	62.2	63.8
PANet [Wang <i>et al.</i> , 2019]	66.5	70.7
CANet [Zhang <i>et al.</i> , 2019]	66.2	69.6
PRNet (ours)	<b>68.79</b>	<b>73.40</b>

Table 4: Binary-IoU results on PASCAL-5<sup>i</sup>.

Methods	Split	1-shot	5-shot
A-MCG [Hu <i>et al.</i> , 2019]	A	52.0	54.7
PANet [Wang <i>et al.</i> , 2019]		59.2	63.5
PRNet (ours)		<b>61.40</b>	<b>64.69</b>
PRNet (ours)	B	<b>65.91</b>	<b>69.37</b>

Table 5: Binary-IoU results on COCO-20<sup>i</sup>.

overfitting in few-shot scenarios. In our experiments, we tune 5 steps for adaptation so as to avoid overfitting.

**Fusion** To demonstrate the effectiveness of our proposed prototype fusion, we show 1-shot results on PASCAL-5<sup>i</sup> in Figure 3. It excludes the step of adaptation for ablation. The results are averaged from 5 runs in each fold. From the curves with a general increasing tendency, we can see that prototype fusion brings in consistent improvement for few-shot segmentation. The first fusion step approximately increases the mean-IoU by 5%. In comparison, the increase boosted in the second fusion step is relatively smaller that is about 1% to 2%. The difference between the two fusion steps can be explained from the visualization in Figure 4.

The visualization of 1-shot segmentation is shown in Figure 4. The third column shows the roughly segmented query images without prototype fusion. It can be seen that segmentation by prototype learning without refinement shows unsatisfactory results, since the prototypes extracted from one support image have limited generality to represent the semantic classes. As expected, our method of prototype fusion is capable of segmenting more precise masks as shown in the last two columns. The first fusion step can segment large positive region of the target class which is wrongly segmented as background before. It is obviously displayed on the *airplane* picture in the two datasets. The second fusion step can refine more details of the target pixels as shown in the last mask of *chair*. As shown in the third column, it segments a clear boundary between *chair* and background after the second fusion step.

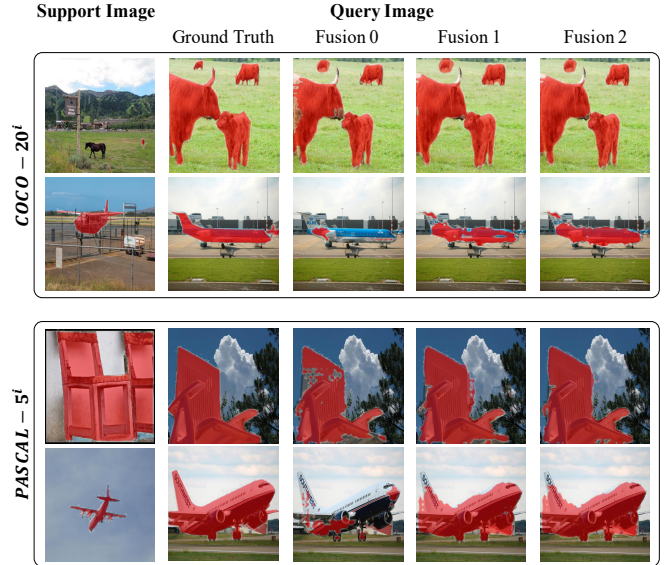


Figure 4: 1-way 1-shot qualitative results of prototype fusion on PASCAL-5<sup>i</sup> and COCO-20<sup>i</sup>. Best viewed in color with zoom.

#### 4.4 2-way Segmentation

Without losing generality, we extend experiments on 2-way tasks on PASCAL-5<sup>i</sup>. We only report the results of prototype fusion in Table 3 for simply illustrating the effectiveness of our method. In each 2-way task, a query image contains at least 1 foreground class. Despite the difficulty in 2-way tasks, we yield the best performance under all evaluation criteria. The results indicate the good generality of our method in higher ways setting. It can be easily extended to N-way K-shot tasks with retaining a comparable performance. Notably, our 2-way mean-IoU scores are even higher than the results that some methods achieve in 1-way settings.

## 5 Conclusions

In this paper, we propose Prototype Refinement Network (PRNet) for few-shot segmentation. PRNet refines class prototypes by adaptation and fusion which make it to be more representative in few-shot scenarios. By simple fusion with support prototypes and query prototypes, we find it effective to bring in significant improvement for segmentation, without importing extra learnable parameters. Comprehensive experiments show the superiority of our method. PRNet consistently outperforms the state-of-the-art methods on COCO-20<sup>i</sup> by large margins of more than 10% and achieves the best result on 2-way segmentation tasks on PASCAL-5<sup>i</sup>.

## References

- [Allen *et al.*, 2019] Kelsey Allen, Evan Shelhamer, Hanul Shin, and Josh Tenenbaum. Infinite mixture prototypes for few-shot learning. In *ICML*, pages 232–241, 2019.
- [Chen *et al.*, 2017] Liang-Chieh Chen, George Papandreou, Florian Schroff, and Hartwig Adam. Rethinking atrous convolution for semantic image segmentation. *arXiv preprint arXiv:1706.05587*, 2017.
- [Chen *et al.*, 2018a] Liang-Chieh Chen, George Papandreou, Iasonas Kokkinos, Kevin Murphy, and Alan L. Yuille. Deeplab: Semantic image segmentation with deep convolutional nets, atrous convolution, and fully connected crfs. *TPAMI*, 40(4):834–848, 2018.
- [Chen *et al.*, 2018b] Liang-Chieh Chen, Yukun Zhu, George Papandreou, Florian Schroff, and Hartwig Adam. Encoder-decoder with atrous separable convolution for semantic image segmentation. In *ECCV*, pages 833–851, 2018.
- [Dhillon *et al.*, 2020] Guneet Singh Dhillon, Pratik Chaudhari, Avinash Ravichandran, and Stefano Soatto. A baseline for few-shot image classification. In *ICLR*, 2020.
- [Dong and Xing, 2018] Nanqing Dong and Eric P. Xing. Few-shot semantic segmentation with prototype learning. In *BMVC*, page 79, 2018.
- [Everingham *et al.*, 2010] Mark Everingham, Luc Gool, Christopher K. Williams, John Winn, and Andrew Zisserman. The pascal visual object classes (voc) challenge. *IJCV*, 88(2):303–338, 2010.
- [Finn *et al.*, 2017] Chelsea Finn, Pieter Abbeel, and Sergey Levine. Model-agnostic meta-learning for fast adaptation of deep networks. In *ICML*, pages 1126–1135, 2017.
- [He *et al.*, 2016] Kaiming He, Xiangyu Zhang, Shaoqing Ren, and Jian Sun. Deep residual learning for image recognition. In *CVPR*, pages 770–778, 2016.
- [Hu *et al.*, 2019] Tao Hu, Pengwan Yang, Chiliang Zhang, Gang Yu, Yadong Mu, and Cees Snoek. Attention-based multi-context guiding for few-shot semantic segmentation. *AAAI*, 33:8441–8448, 2019.
- [Lin *et al.*, 2014] Tsung-Yi Lin, Michael Maire, Serge Belongie, Lubomir Bourdev, Ross Girshick, James Hays, Pietro Perona, Deva Ramanan, C. Lawrence Zitnick, and Piotr Dollár. Microsoft coco: Common objects in context. *arXiv preprint arXiv:1405.0312*, 2014.
- [Lin *et al.*, 2017] Guosheng Lin, Anton Milan, Chunhua Shen, and Ian Reid. Refinenet: Multi-path refinement networks for high-resolution semantic segmentation. In *CVPR*, pages 5168–5177, 2017.
- [Long *et al.*, 2015] Jonathan Long, Evan Shelhamer, and Trevor Darrell. Fully convolutional networks for semantic segmentation. In *CVPR*, pages 3431–3440, 2015.
- [Nguyen and Todorovic, 2019] Khoi Nguyen and Sinisa Todorovic. Feature weighting and boosting for few-shot segmentation. In *ICCV*, pages 622–631, 2019.
- [Nichol and Schulman, 2018] Alex Nichol and John Schulman. Reptile: a scalable metalearning algorithm. *arXiv: Learning*, 2018.
- [Rakelly *et al.*, 2018] Kate Rakelly, Evan Shelhamer, Trevor Darrell, Alyosha A. Efros, and Sergey Levine. Conditional networks for few-shot semantic segmentation. In *ICLR (Workshop)*, 2018.
- [Ronneberger *et al.*, 2015] Olaf Ronneberger, Philipp Fischer, and Thomas Brox. U-net: Convolutional networks for biomedical image segmentation. In *MICCAI*, pages 234–241, 2015.
- [Russakovsky *et al.*, 2015] Olga Russakovsky, Jia Deng, Hao Su, Jonathan Krause, Sanjeev Satheesh, Sean Ma, Zhiheng Huang, Andrej Karpathy, Aditya Khosla, Michael Bernstein, Alexander C. Berg, and Li Fei-Fei. ImageNet large scale visual recognition challenge. *IJCV*, 115(3):211–252, 2015.
- [Shaban *et al.*, 2017] Amirreza Shaban, Shray Bansal, Zhen Liu, Irfan Essa, and Byron Boots. One-shot learning for semantic segmentation. In *BMVC*, 2017.
- [Siam *et al.*, 2019] Mennatullah Siam, Boris N Oreshkin, and Martin Jagersand. Amp: Adaptive masked proxies for few-shot segmentation. In *ICCV*, pages 5249–5258, 2019.
- [Simonyan and Zisserman, 2015] Karen Simonyan and Andrew Zisserman. Very deep convolutional networks for large-scale image recognition. In *ICLR*, 2015.
- [Snell *et al.*, 2017] Jake Snell, Kevin Swersky, and Richard Zemel. Prototypical networks for few-shot learning. In *NIPS*, pages 4077–4087, 2017.
- [Wang *et al.*, 2019] Kaixin Wang, JunHao Liew, Yingtian Zou, Daquan Zhou, and Jiashi Feng. Panet: Few-shot image semantic segmentation with prototype alignment. *arXiv preprint arXiv:1908.06391*, 2019.
- [Yu and Koltun, 2016] Fisher Yu and Vladlen Koltun. Multi-scale context aggregation by dilated convolutions. In *ICLR*, 2016.
- [Zhang *et al.*, 2018] Xiaolin Zhang, Yunchao Wei, Yi Yang, and Thomas Huang. Sg-one: Similarity guidance network for one-shot semantic segmentation. *arXiv preprint arXiv:1810.09091*, 2018.
- [Zhang *et al.*, 2019] Chi Zhang, Guosheng Lin, Fayao Liu, Rui Yao, and Chunhua Shen. Canet: Class-agnostic segmentation networks with iterative refinement and attentive few-shot learning. In *CVPR*, pages 5217–5226, 2019.